SAND2016-4035J

Nonlinear dynamics and instability of aqueous dissolution of silicate glasses and minerals

Yifeng Wang[1]*, Carlos F. Jove-Colon[1] and Kristopher L. Kuhlman[1]

[1]Sandia National Laboratories, P. O. Box 5800, Albuquerque, New Mexico 87185-0779, USA
E-mail: ywang@sandia.gov

Aqueous dissolution of silicate glasses and minerals plays a critical role in global biogeochemical cycles and climate evolution[1-2]. The reactivity of these materials is also important to numerous engineering applications including nuclear waste disposal[3-4]. The dissolution process has long been considered to be controlled by a leached surface layer in which cations in the silicate framework are gradually leached out and replaced by protons from the solution[5,6]. This view has recently been challenged by observations of extremely sharp corrosion fronts and oscillatory zonings in altered rims of the materials[7-9], suggesting that corrosion of these materials may proceed directly through congruent dissolution followed by secondary mineral precipitation. Here we show that complex silicate material dissolution behaviors can emerge from a simple positive feedback between dissolution-induced cation release and cation-enhanced dissolution kinetics. This self-accelerating mechanism enables a systematic prediction of the occurrence of sharp dissolution fronts (vs. leached surface layers), oscillatory dissolution behaviors and multiple stages of glass dissolution (especially alteration resumption at a late stage of a corrosion process). Our work provides a new perspective for predicting long-term silicate weathering rates in actual geochemical systems and developing durable silicate materials for various engineering applications.

Despite decades of intensive research, the mechanism controlling aqueous dissolution of silicate materials still remains controversial[4,6,7]. The debate has centered on the possible formation of a leached surface layer and its role in material dissolution. A silica-rich surface layer has been detected on both manufactured and natural silicate materials[5,10,11]. Alkali and alkaline cations in this layer are partially leached out and replaced by hydrogen ions through a coupled diffusion-ion exchange process. The leached layer may be subjected to *in-situ* silicate network reorganization, leading to the formation of a dense silica gel layer that may passivate a dissolving solid surface[3,6]. However, this view has been challenged by recent observations of extremely sharp interfaces between altered rims and pristine material domains[7,8, 12] and oscillatory zonings in the altered rims (Figure 1A)[7,9,13,14], suggesting that material corrosion may undergo a direct dissolution-precipitation process[7,8]. Temporal oscillations in silicate dissolution have been observed in laboratory experiments[15-17]. The contradicting observations clearly indicate the complexity of silicate material dissolution and call for a new theory to account for such complexity. The new theory must also explain the multiple stages of a glass dissolution process (Figure 2A). As a silicate glass corrodes, the corrosion rate generally decreases, due to the reduction in chemical affinity for silicate network dissolution and the formation of a passivating layer on glass surfaces[3,4,6]. Interestingly, a sharp increase in corrosion rate after a long period of rate drop has often been observed in silicate glass dissolution experiments[18,19]. The underlying mechanism for this remains unknown[4].

Oscillatory zonings on archeologic glass samples have been attributed to seasonal fluctuations in temperature or hydrologic conditions[20]. But this explanation is apparently not applicable to laboratory experiments, which are usually conducted under static conditions with no externally imposed periodic changes on experimental conditions[9,13]. Thus, the observed oscillatory dissolution behaviors must be self-organizational[13], i.e., originated from the internal dynamics of solid-water interactions. Self-organization requires a positive feedback among physical and chemical processes involved in a system[21,22]. In silicate material dissolution, the following positive feedback exists: As a silicate material corrodes, cations (notably Na^+) in the material are released into the solution, resulting in a local high cation concentration

and pH at the reaction front ($\Delta[OH^-] \approx \Delta[cation]$ for charge balance). Under alkaline conditions, silicate dissolution is catalyzed by both hydroxyl groups and cations[23-25]. The resultant high pH and cation concentration enhance silicate material dissolution, which in turn accelerates cation release. A silicate dissolution rate usually has a V-shape dependence on pH (ref. 23). The proposed self-accelerating mechanism operates only under alkaline conditions, that is, on the right branch of the rate curve in Figure 2B.

We formulated a nonlinear dynamic model for glass dissolution (see equations and nomenclatures in Methods). Numerical simulations of the model show that the proposed mechanism generates oscillatory dissolution (Figure 3). The equilibrium silica concentration for glass dissolution is estimated to be ~ 10^{-3} to 10^{-2} M (ref. 26). The cation concentration at the isoelectric point (IEP) (C_{IEP}) (Figure 2B) can vary widely depending on experimental or environmental conditions; a range of 10^{-4} to 10^{-2} M could be a reasonable choice[15]. Accordingly, the concentration ratio between silica and cation (θ) in Figure 3A varies from 1 to 100. Oscillatory dissolution occurs over a wide range of θ but only within a narrow range (0.8 to 3.0) of γ. The narrow γ range implies that self-organization requires the dissolution rate and the mass exchange rate to be on the same order of magnitude so that the two processes can interplay with each other. At the beginning of the dissolution, no altered zone is developed and the dissolution process is overwhelmed by mass exchange. Thus, γ always starts from a low value, and then increases as the alteration product builds up, leading to a transition from a plain altered zone to an oscillatory zone (Figure 4A), as observed[9,13]. Self-organization also requires the order of the dissolution reaction with respect to cation to be higher than 1.4 (Figure 4B). The dissolution rate is known to be proportional to $[\equiv OH^-]^2$ (refs. 27 and 28), where $[\equiv OH^-]$ is the adsorbed hydroxyls. At low surface coverages, $[\equiv OH^-] \propto [OH^-]$. Considering the additional catalytic effect of cations through ionic strength[25], the reaction order n is estimated to be ~ 1.0 to 2.5. Parameter α is determined by glass composition and constrained between 0.3 and 0.6 (refs. 11 and 16). Oscillatory dissolution is thus expected to be relatively common in silicate material corrosion (Figure 4).

The time scale for each oscillation (T_b) is estimated to be (See methods):

$$T_b \approx \tau_b T = \tau_b \frac{L_1 L_2}{D_c} \tag{1}$$

where τ_b is the scaled time for each oscillation, estimated to be 10 – 50 from the numerical simulations. The thicknesses of the boundary layer (L_1) and the altered zone (L_2) are chosen to be ~ 1 and ~10 μm (ref. 13), respectively. The diffusion in the altered zone (D_c) in a reorganized dense silica gel could be as low as 6×10^{-15} cm^2/s (ref. 6). As discussed below, such a dense layer is unlikely to form under the conditions for oscillatory dissolution, and the altered zone could be porous[13]. D_c is thus chosen to be 10^{-14} to 10^{-12} cm^2/s. From Equation (1), the time scale for each oscillation is estimated to range from hours to a year, consistent on observations[9,13,20]. Similarly, the thickness of each band (L_b) can be estimated by (see Methods):

$$L_b \approx \gamma v_m C_{\mathrm{IEP}}(1 + \beta \bar{c}^n) L_1 \tag{2}$$

where $\bar{c}$ is a typical scaled cation concentration chosen to be ~ 10 based on the numerical simulations; and v_m is the volume of pristine solid containing 1 mole of SiO_2, estimated to be ~30 cm^3/mole. For $\gamma \approx 1.0$, $\beta \approx 5$ (Figures 3 and 4) and C_{IEP} = 10^{-4} to 10^{-2} M (see the discussion above), L_b is estimated to range from $0.1L_1$ to a few L_1 units. A gap of micrometers has been observed between the pristine glass surface and

the altered rim[13]. If we take this gap as the boundary layer, the scale of each band is estimated to be sub-micrometers to micrometers, consistent with observations[8,13].

The proposed mechanism provides a logical explanation for the occurrence of leached layers. The evolution of the leached layer thickness (L_g) is governed by (see Methods for nomenclatures):

$$\frac{dL_g}{dt} \approx \frac{D_g}{L_g} - Rv_m = \frac{D_g}{L_g} - v_m k_d C_{\mathrm{IEP}}(S_d^e - S)\left[1 + \beta\left(\frac{D_g L_2}{C_{\mathrm{IEP}} L_g}\right)^n\right] \quad (3)$$

where D_g is the cation diffusion coefficient in the leached layer. For the reaction order $n > 1$, as material dissolution pushes the chemistry of the boundary layer toward the right branch of the dissolution curve in Figure 2B and the reaction product builds up (increasing L_2), the second term in the far right-hand side would eventually overtake the first term, and the leached layer then becomes progressively thinner – a self-sharpening mechanism for the formation of an extremely sharp interface between a pristine silicate material and the surrounding altered rim[8,13]. Leached layers are transient, which tend to form at an early stage of a dissolution process under mildly acid to neutral conditions (the lower part of the dissolution curve in Figure 2B).

The stage of alteration resumption is also a consequence of the self-accelerating mechanism. Assume that glass dissolution starts on the lower part of the dissolution curve in Figure 2B. Due to a low dissolution rate, a leached layer forms. As the dissolution proceeds, the dissolution rate increases as more cations accumulate in the boundary layer, leading to disappearance of the leached layer. When the dissolution rate becomes on the same order of magnitude as the mass exchange rate with the bulk solution, oscillatory dissolution may emerge. Eventually, the dissolution rate overtakes the mass exchange rate, leading to a "runaway" situation with a sharp increase in the cation concentration at the interface and therefore the dissolution rate. The sharp increase in both cation concentration and pH inevitably causes zeolite precipitation (Figure S1). Contradicting the existing view that the zeolite precipitation would be a cause for alteration resumption[26], our work suggests that zeolite formation is a consequence of the alteration resumption process, consistent with experimental observations[29]. The precipitation of zeolite would eventually limit further increase in the reaction rate by removing cations from the boundary layer (Figure S1). Thus, the resumption rate may represent a long-term rate for silicate glass dissolution. Whether or how soon the alteration resumption occurs depends on glass composition. The durability of a glass can thus be improved by choosing an appropriate glass composition such that a proper alteration product will form which will limit the dissolution to the lower part of the dissolution curve (Figure 2B).

The proposed mechanism provides a new perspective for predicting silicate mineral weathering rates in natural systems. The pH and cation concentration of water at a dissolution interface could be much higher than those in the bulk solution (e.g. extractable pore water). Using pore water chemistry for prediction, as done currently, may significantly underestimate mineral reaction rates. Similarly, silicate mineral weathering in environments with limited water availability, for example, in semiarid to arid regions, may be more dynamic than previously thought. The proposed mechanism could create local high pH microenvironments and thus enhance CO_2 dissolution and mineralization, a mechanism probably responsible for large CO_2 uptake by desert soils[30].

Methods

The modeling system for oscillatory silicate glass dissolution is shown in Figure 1B. It consists of three physical domains: a pristine glass domain, a boundary layer, and an alteration zone. The leached layer in the figure is not included, because it is likely to be absent in oscillatory dissolution due to the

self-sharpening effect of a reaction front as discussed above. The dynamics of aqueous silicate material dissolution can be described by:

$$L_1 \frac{dC\prime}{dt} = \alpha k_d C_{\text{IEP}} \left[1 + \beta \left(\frac{C\prime}{C_{\text{IEP}}}\right)^n\right](S_d^e - S') - \frac{D_c}{L_2}(C' - C_0) \quad (4)$$

$$L_1 \frac{dS'}{dt} = \alpha k_d C_{\text{IEP}} \left[1 + \beta \left(\frac{C'}{C_{\text{IEP}}}\right)^n\right](S_d^e - S') - \frac{D_s}{L_2}(S' - S_0) - k_p(S' - S_p^e) \quad (5)$$

where

C' – Cation concentration within the boundary layer
C_0 – Cation concentration in the bulk solution (outside the altered zone)
D_c – Diffusion efficient of cations in the altered zone
D_s – Diffusion coefficient of dissolved silica in the altered zone
L_1 – Thickness of the boundary layer at the dissolution interface
L_2 – Thickness of the altered zone
k_d – Reaction rate constant for silicate material dissolution
k_p – Reaction rate constant for silica mineral precipitation
n – Order of silicate dissolution reaction with respect to cation
S' – Silica concentration within the boundary layer
S_0 – Silica concentration in the bulk solution
S_d^e – Equilibrium silica concentration for material dissolution
S_p^e – Equilibrium silica concentration for silica precipitation
t – Time
α – Molar ratio of cations (mainly Na^+) to Si^{4+} in the pristine silicate material
β – Positive constant characterizing the catalytic effect of cations on silicate material dissolution

The first terms on the right-hand side of Equations (4) and (5) represent the mass accumulation due to silicate material dissolution. The factor $\left[1 + \beta \left(\frac{C\prime}{C_{IEP}}\right)^n\right]$ is introduced to capture the catalytic effect of cations on the dissolution of silicate network in the materials. We here only consider silicate material dissolution under alkaline conditions, that is, on the right branch of the dissolution curve in Figure 2B. The dissolution reaction is assumed to be first order with respect to the dissolved silica concentration[26]. The other terms on the right-hand side of the equations represent the mass exchange between the boundary layer and the bulk solution or the mass consumption by silica mineral precipitation.

Equations (4) and (5) can then be cast into the following dimensionless equations:

$$\frac{dc}{d\tau} = \alpha\gamma(1 + \beta c^n)(1 - s) - (c - c_0) \quad (6)$$

$$\theta \frac{ds}{d\tau} = \gamma(1 + \beta c^n)(1 - s) - \eta(s - s_0) - \kappa(s - s_p) \quad (7)$$

With the following scaling factors:

$$c = \frac{C'}{C_{\text{IEP}}} \qquad s = \frac{S'}{S_d^e} \qquad \tau = \frac{t}{T}$$

$$T = \frac{L_1 L_2}{D_c} \qquad \gamma = \frac{k_d S_d^e L_2}{D_c} \qquad \theta = \frac{S_d^e}{C_{\mathrm{IEP}}} \qquad (8)$$

$$\eta = \frac{D_s S_d^e}{D_c C_{\mathrm{IEP}}} \qquad \kappa = \frac{k_p S_d^e L_2}{D_c C_{\mathrm{IEP}}}$$

where

c - Scaled silica concentration
s – Scaled silica concentrations
T – Typical time scale of the system
γ – Scaled glass dissolution rate relative to the rate of diffusional mass exchange between the boundary layer and the bulk solution
η – Scaled diffusivity ratio between silica and cation
θ – Typical concentration ratio between silica and cation
κ – Scaled rate constant for silica mineral precipitation
τ – Scaled time

Equations (6) and (7) were solved using an arbitrary ordinary differential equation solver from python package mpmath (http://mpmath.org/) and Mathematica (Wolfram Research Inc. 2015). The behavior diagrams in Figure 4 were constructed by numerical simulations.

Acknowledgements: Sandia National Laboratories is a multi-program laboratory managed and operated by Sandia Corporation, a wholly owned subsidiary of Lockheed Martin Corporation, for the U.S. Department of Energy's National Nuclear Security Administration under contract DE-AC04-94AL85000. The work was supported by DOE Used Fuel Disposition (UFD) Program and by an Energy Frontier Research Center (EFRC) funded by the U.S. Department of Energy (DOE), Office of Sciences (BES).

References

1. Berner, R. A. & Kothavala, Z. GEOCARB III: A revised model of atmospheric CO_2 over Phanerozoic time. *Am. J. Sci.* **301**, 182-204 (2001).
2. Brady, P. V. The effect of silicate weathering on global temperature and atmospheric CO_2. *J. Geophysical Lett*. **96**, 18101-18106 (1991).
3. Cailleteau, C. et al. Insight into silicate-glass corrosion mechanisms. *Nature Materials* **7**, 978-983 (2008).
4. Gin, S. Open scientific questions about nuclear glass corrosion. *Procedia Materials Sci.* **7**, 163-171 (2014).
5. Dran, J.-C., Petit, J.-C., Brousse, C. Mechanism of aqueous dissolution of silicate glasses yield by fission tracks. *Nature* **319**, 485-487 (1986).
6. Gin, S. et al. Origin and consequences of silicate glass passivation by surface layers. *Nature Communications* **6**, 6360 doi: 10.1038/ncomms7360 (2015).
7. Putnis, A. Sharpened interface. *Nature Materials* **14**, 261-261 (2015).
8. Hellmann, R. et al. Nanometre-scale evidence for interfacial dissolution-reprecipitation control of silicate glass corrosion. *Nature Materials* **14**, 307-311 (2015)
9. Geisler, T. et al. Aqueous corrosion of borosilicate glass under acidic conditions: A new corrosion mechanism. *J. Non-Crystalline Solids* **356**, 1458-1465 (2010).
10. Doremus, R. H. Interdiffusion of hydrogen and alkali ions in a glass surface. *J. Non-Crystalline Solids* **19**, 137-144 (1975).

11. Petit, J.-C. et al. Hydrated-layer formation during dissolution of complex silicate glasses and minerals. *Geochim. Cosmochim. Acta* **54**, 1941-1955 (1990).
12. Ruiz-Agudo, E. et al. Mechanism of leached layer formation during chemical weathering of silicate minerals. *Geology* **40**, 947-950 (2012).
13. Dohmen, L. et al. Pattern formation in silicate glass corrosion zones. *Int. J. Appl. Glass Sci.* **4**, 357-370 (2013).
14. Jeong, G. Y. & Sohn, Y. K. Mineralogy and microtextures of basaltic glass alteration in hyaloastite, Jeju Island, Korea. *J. Analytical Sci. Tech.* **2**, 12-22 (2011).
15. Falmon, J. Oscillatory silicon and aluminum aqueous concentrations during experimental aluminosilicate weathering. *Geochim. Cosmochim. Acta* **60**, 2901-2907 (1996).
16. Barkatt, A., Sang, J. C. & Jakubik, R. F. Oscillations in the dissolution kinetics of silicate glass in tri-buffered aqueous media. *J. Non-Crystalline Solids* **155**, 141-148 (1993).
17. Leturcq, G., Berger, G., Advocat, T. & Vernaz, E. Initial and long-term dissolution rates of aluminosilicate glasses enriched with Ti, Zr and Nd. *Chemical Geology* **160**, 39-62 (1999).
18. Neeway J. J. et al. *A Strategy to Conduct an Analysis of the Long-Term Performance of Low-Activity Waste Glass in a Shallow Subsurface Disposal System at Hanford*. Pacific Northwest National Laboratory, Richland, Washington, PNNL-23503 (2014).
19. Fournier, M., Frugier, P. & Gin, S. Resumption of alteration at high temperature and pH: rates measurements and comparison with initial rates. *Procedia Materials Sci.* **7**, 202-208 (2014).
20. Brill, R. H. & Hood, H. P. A new method for dating ancient glass. *Nature* **189**, 12-14 (1961).
21. Nicolis, G. & Prigogine, I. *Self-organization in Non-Equilibrium Systems* (Wiley, New York, 1977).
22. Wang, Y. Xu, H., Merino, E. & Konishi, H. Generation of banded iron formation by internal dynamics and leaching of oceanic crust. *Nature Geoscience* **2**, 781-784 (2009).
23. Stumm, W. Chemistry of the Solid-Water Interface: Processes at the Mineral-Water and Particle-Water Interface in Natural Systems (Wiley, New York, 1992).
24. Wolery, W. G., Tester, J. W. & Grigsby, C. O. Quartz dissolution kinetics from 100-200 oC as a function of pH and ionic strength. AIChE J. 42, 3442-3457 (1996).
25. Icenhower, J. P. & Dove, P. M. The dissolution kinetics of amorphous silica into sodium chlorite solutions: Effects of temperature and ionic strength. *Geochim. Cosmochim. Acta* **64**, 4193-4203 (2000).
26. Gin, S. et al. Effect of composition on the short-term dissolution rates of ten borosilicate glasses of increasing complexity from 3 to 30 oxides. *J. Non-Crystalline Solids* **358**, 2559-2570 (2012).
27. Wieland, R., Wehrli, B. & Stumm, W. The coordination chemistry of weathering: III. A generalization on the dissolution rates of minerals. *Geochim. Cosmochim. Acta* **52**, 1969-1981 (1988).
28. Wirth, G. S. & Gieskes, J. M. The initial kinetics of the dissolution of vitreous silica in aqueous media. *J. Colloid Interface Sci.* **68**, 492-500 (1979).
29. Fournier, M., Frugier, P. & Gin, S. Effect of zeolite formation on borosilicate glass dissolution kinetics. *Procedia Earth Planet. Sci.* **7**, 264-267 (2013).
30. Wohlfahrt, G., Fenstermaker, L. F. & Arone III, J. A. Large annual net ecosystem CO_2 uptake of a Mojave Desert ecosystem. *Global Change Biology* **14**, 1475-1487 (2002).

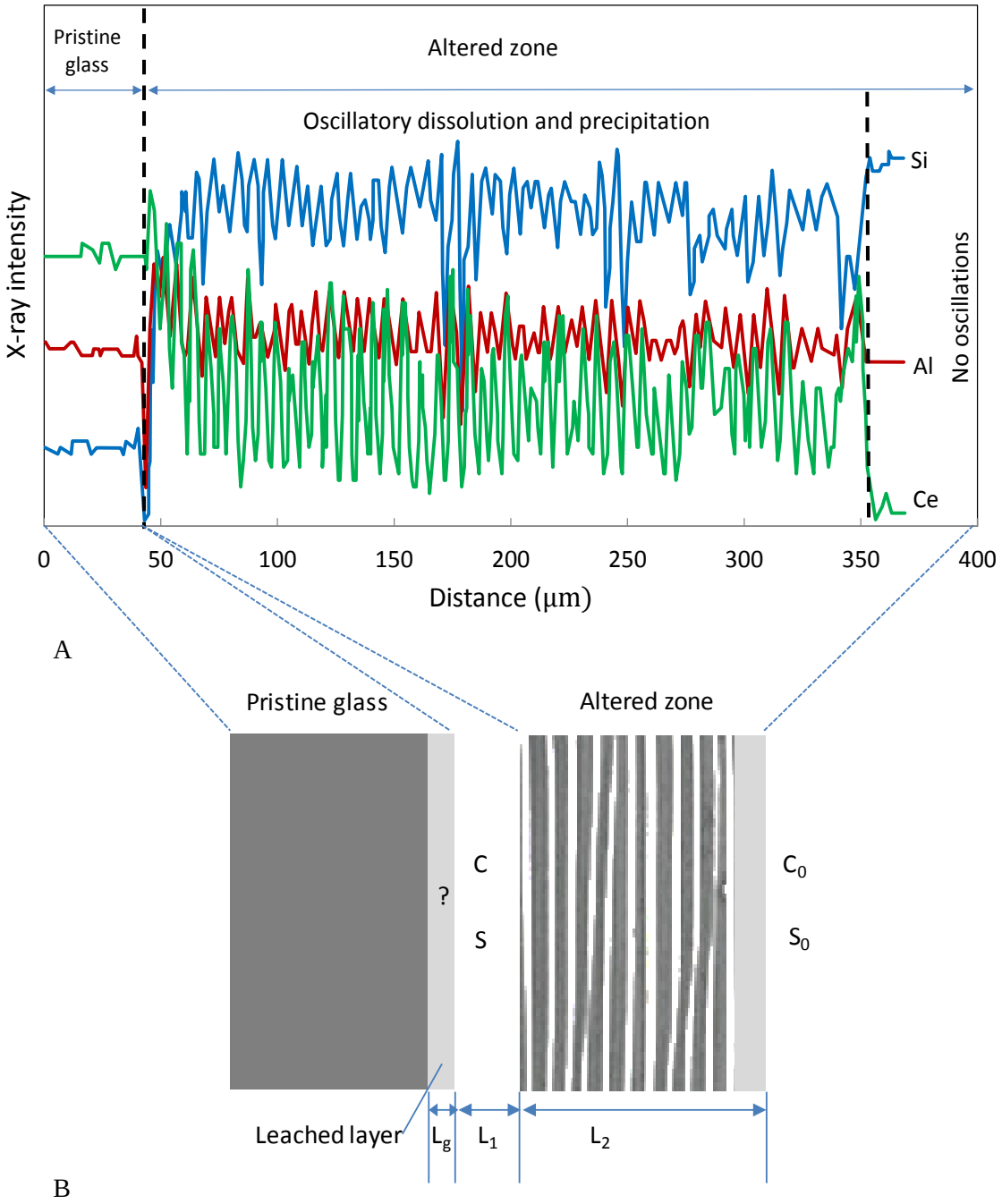

Figure 1| Oscillatory borosilicate glass dissolution and mineral precipitation as indicated by compositional zoning in an alteration zone (A) and schematic representation of modeling system (B). Data in (A) were taken from reference 9.

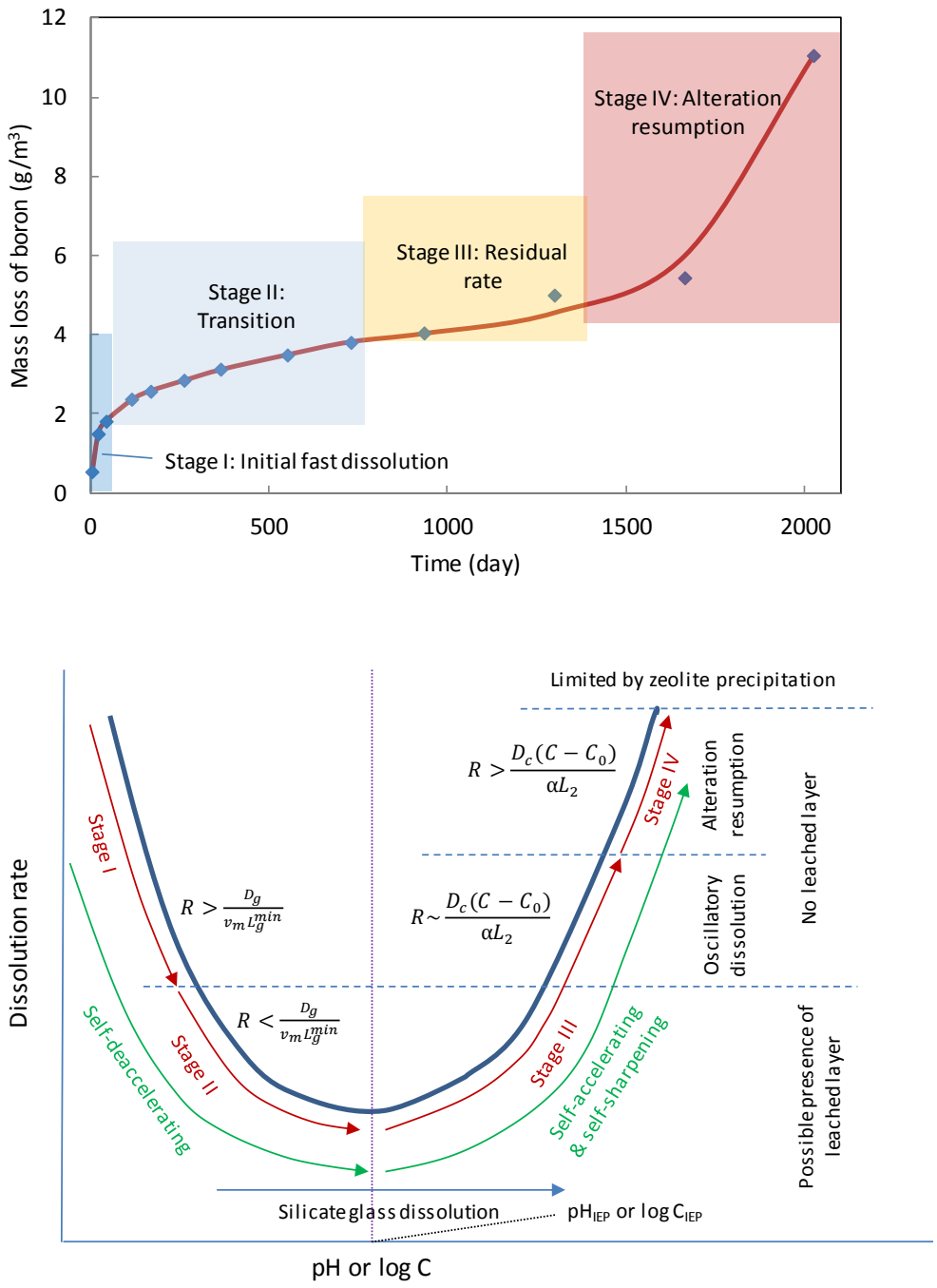

Figure 2| Evolution of silicate glass dissolution (A) and its nonlinear dynamics (B). A positive feedback between glass dissolution and solution chemistry may lead to oscillatory glass dissolution, interface sharpening and alteration resumption at the late stage of glass corrosion. Note that this feedback becomes effective only for the base leg of the dissolution curve (B). IEP: Isoelectric point. L_g^{min} is the minimum spatial resolution for a microanalysis and imaging technique for characterizing the sharpness of a reaction front (≤ 1nm). The data points in (A) were taken from reference 18.

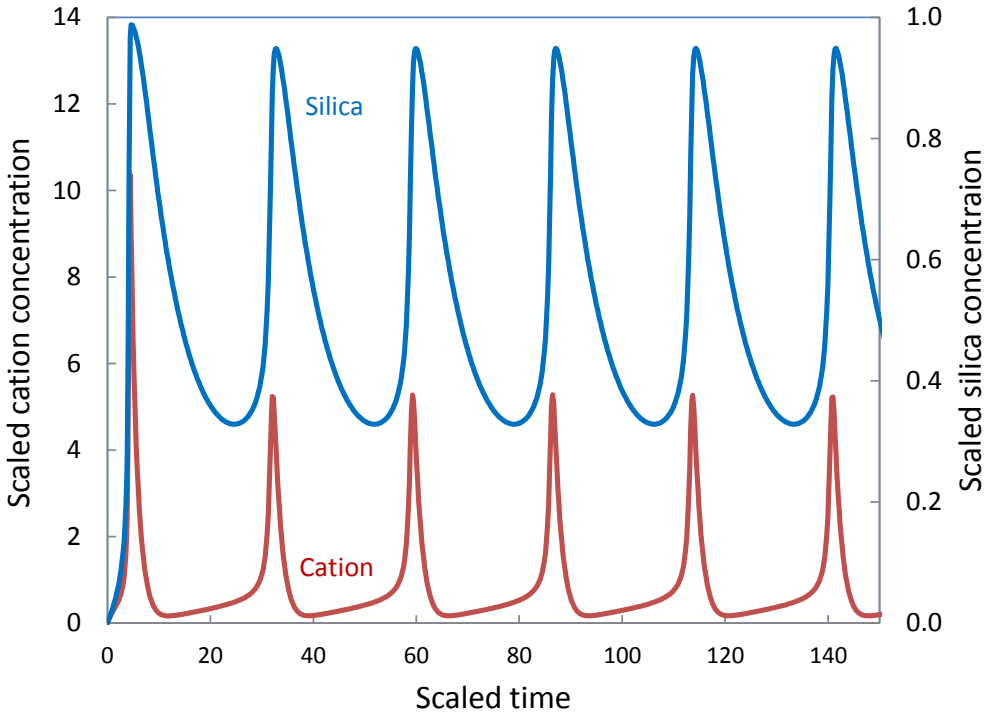

Figure 3| Predicted concentration oscillations at the glass dissolution interface. Parameter values used in the simulation**:** α = 0.4, γ = 0.9, n = 2.0, β = 5.0, θ = 40, η = 2, κ = 2.0, $c_0 = s_0 = s_p^e$ = 0.001 (see Methods for parameter definitions).

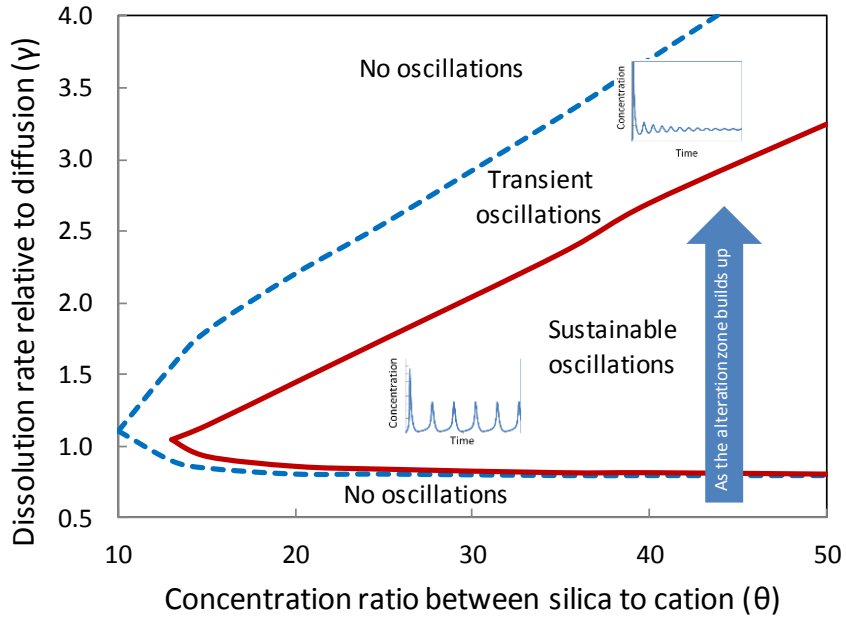

A

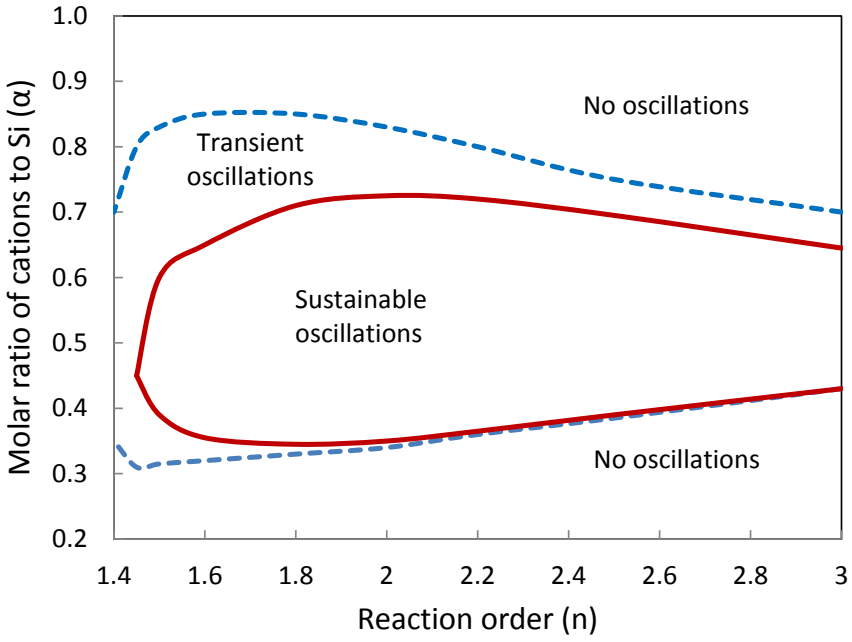

B

Figure 4| Behavior diagrams for silicate glass dissolution. As the alteration zone builds up, the dissolution transits from a no-oscillation state to an oscillation state as observed (Geisler et al., 2010). Parameter values used in the calculation**:** (A) α = 0.4, n = 2.0, β = 0.9, η = 2, κ = 2.0, c_0 = s_0 = s_p^e = 0.001; (B) γ = 1.0, n = 2.0, β = 1.0, θ = 40, κ = 2.0, c_0 = s_0 = s_p^e = 0.001 (see Methods for parameter definitions).

Supplementary information

Nonlinear dynamics and instability of aqueous dissolution of silicate glasses and minerals

Yifeng Wang[1]*, Carlos F. Jove-Colon[1] and Kristopher L. Kuhlman[1]

[1]Sandia National Laboratories, P. O. Box 5800, Albuquerque, New Mexico 87185-0779, USA
E-mail: ywang@sandia.gov

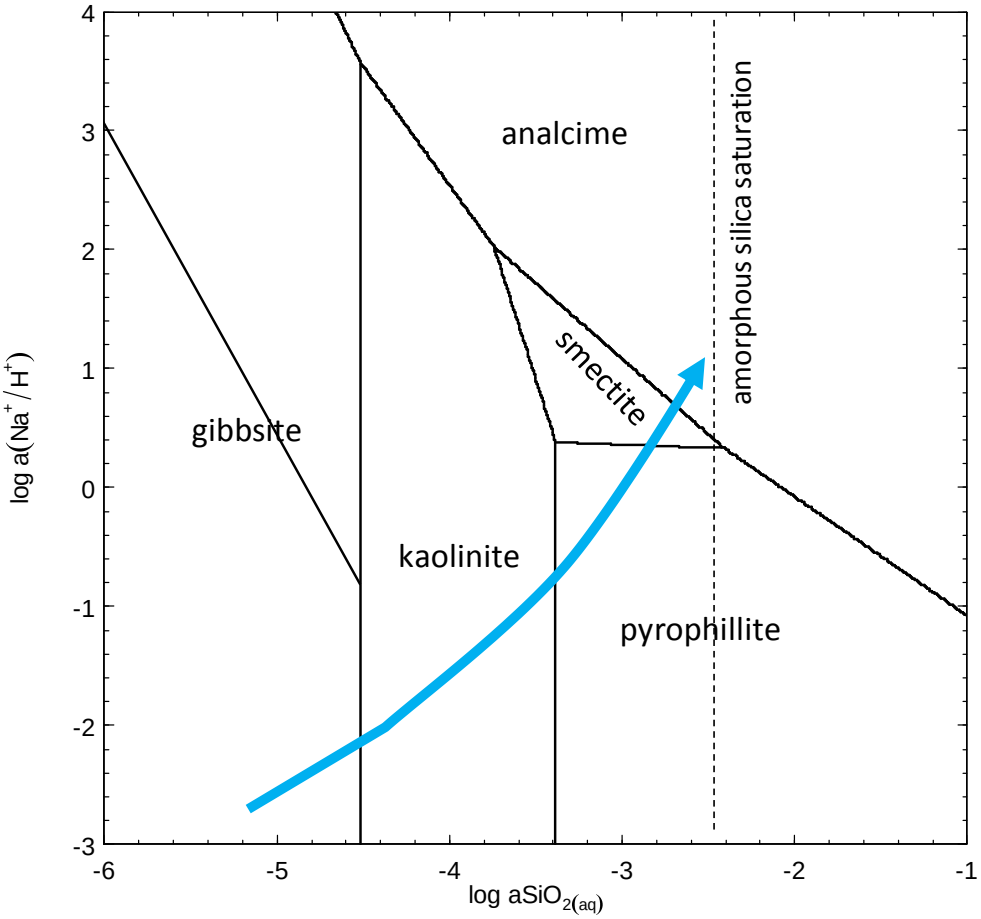

Figure S1| Evolution of water chemistry and mineral precipitation at a reaction front of silicate material dissolution. Sources of thermodynamic data: Kaolinite - Blanc, P., A. Lassin, P. Piantone, M. Azaroual, N. Jacquemet, A. Fabbri, and A. Gaucher, Thermoddem: A geochemical database focused on low temperature water/rock interactions and waste materials. Applied Geochemistry, 2012. 27: p. 2107-2116. Smectite MX80 - Blanc, P., A. Lassin, P. Piantone, M. Azaroual, N. Jacquemet, A. Fabbri, and A. Gaucher, Thermoddem: A geochemical database focused on low temperature water/rock interactions and

waste materials. Applied Geochemistry, 2012. 27: p. 2107-2116. Gibbsite - (1) Tutolo, B.M., X.-Z. Kong, W.E. Seyfried, Jr., and M.O. Saar, Internal consistency in aqueous geochemical data revisited: Applications to the aluminum system. Geochim. Cosmochim. Acta, 2014. 133: p. 216-234. Or Robie, R.A. and B.S. Hemingway, Thermodynamic properties of minerals and related substances at 298.15 K and 1 bar (10^5 pascals) pressure and at higher temperatures. U S Geological Survey bulletin 2131, 461 pp. Analcime - Neuhoff, P.S., G.L. Hovis, G. Balassone, and J.F. Stebbins, Thermodynamic properties of analcime solid solutions. Am. J. Sci., 2004. 304(1): p. 21-66. Pyrophillite: Tutolo, B.M., X.-Z. Kong, W.E. Seyfried, Jr., and M.O. Saar, Internal consistency in aqueous geochemical data revisited: Applications to the aluminum system. Geochim. Cosmochim. Acta, 2014. 133: p. 216-234.